

Laser bandwidth effects in quantitative cavity ring-down spectroscopy

Joseph T. Hodges, J. Patrick Looney, and Roger D. van Zee

We have investigated the effects of laser bandwidth on quantitative cavity ring-down spectroscopy using the ν_R transitions of the $b(\nu = 0) \leftarrow X(\nu = 0)$ band of molecular oxygen. It is found that failure to account properly for the laser bandwidth leads to systematic errors in the number densities determined from measured ring-down signals. When the frequency-integrated expression for the ring-down signal is fitted and measured laser line shapes are used, excellent agreement between measured and predicted number densities is found.

Recent advances in optical technology have precipitated the development of new spectroscopic techniques, of which cavity ring-down spectroscopy (CRDS) is one of the most promising for quantitative trace-gas measurements.¹⁻⁵ The centerpiece of the CRDS technique is a high- Q , two-mirror stable resonator into which laser light is injected through one end mirror. While this mirror reflects most of the incident light, a small fraction couples into the cavity and rings down exponentially in time, with the time decay determined by the mirror losses. When a gaseous species is introduced into the cavity and the laser is tuned to an absorption resonance, the ring-down time is reduced. From the reduction in the time constant, the number density of the absorbing species can be determined. With state-of-the-art mirrors and lasers,⁶ absorptivities of less than 10^{-10} cm^{-1} should be detectable.

Several experimental factors, such as mode matching, mirror quality, and laser line shape, complicate realization of the ultimate theoretical detection sensitivity. Of these factors, the effect of the laser's spectral content has yet to be fully considered. This subject is explored below by the use of the ν_R transitions of the $b(\nu = 0) \leftarrow X(\nu = 0)$ band of O_2 (the A band), which is a band that has been well characterized spectroscopically.⁷⁻⁹ This paper demonstrates the effect of the laser's spectral content on the ring-down signal, models the observed effects, and

argues that truly quantitative measurements are best done with a narrow line laser with a well-characterized spectrum.

Two sets of experiments were carried out with laser systems with different spectral properties. One system¹⁰ was a $\text{Nd}^{3+}:\text{YAG}$ (Continuum NY61-10; ~ 7 -ns pulse duration; 10 Hz) pumped dye laser (Spectra-Physics PDL-3; dye LDS 759), which generated radiation consisting of as many as 11 longitudinal modes [each of ~ 200 -MHz half-width at half-maximum (HWHM)] separated by ~ 480 MHz. The other was a $\text{Nd}^{3+}:\text{YAG}$ pumped $\text{Ti}:\text{Al}_2\text{O}_3$ laser (STI Optronics HRL-50C), which produced single-mode radiation with a time-integrated bandwidth of ~ 175 – 200 -MHz HWHM. A unit magnification spatial filter assembly containing a 70 - μm diamond pinhole was used to provide a nearly collimated, axisymmetric beam. To minimize the effects of amplified spontaneous emission from the dye laser and fluorescence from the $\text{Ti}:\text{Al}_2\text{O}_3$ laser, a dielectric notch filter ($765 \pm 6 \text{ nm}$) was placed in front of the cavity. The spectral output from these lasers was measured with an étalon with a 10-GHz free spectral range and a resolution of 100 MHz. The ring-down cavity used in these experiments was a 118-cm-long stainless-steel tube fitted with 1-m radius-of-curvature mirrors on both ends [Newport SR40F; total losses ~ 2000 parts in 10^6 (ppm) per pass]. Successful alignment of the cavity was confirmed by the measurement of the spatial structure of the light that leaked out of the cavity (on the end opposite to the laser injection) with a CCD array camera. Light was injected into the cavity off axis and aligned to a two-spot pattern.¹¹ To measure ring-down signals, the CCD array camera was replaced with a low-gain, near-infrared photomultiplier tube (Hamamatsu

R1913) preceded by a glass diffuser. The output signal was terminated into 50 Ω and digitized by an 8-bit, 100-Msample/s digital oscilloscope (LeCroy 9310). The effective bandwidth of the detection system was ~ 30 MHz. For further data processing, individual ring-down traces were downloaded from the oscilloscope by a personal computer. Scientific-grade O_2 (MG Scientific; specified purity 99.999%) was used without further purification. The data reported here were collected at ~ 1333 Pa (~ 10 Torr) and room temperature (~ 296 K). The O_2 line shape under these conditions was essentially Doppler broadened (~ 430 -MHz HWHM), with a residual amount of pressure broadening (~ 40 -MHz HWHM) and was well represented by a Voigt profile with ~ 450 -MHz HWHM.⁹ Accurate and precise temperature (≈ 0.01 K) and pressure measurements ($\pm 0.5\%$) were made with a Pt resistance thermometer and capacitance diaphragm gauge, respectively, both of which were calibrated against standards maintained at the National Institute of Standards and Technology.

As formulated by Zalicki and Zare,⁴ the time-dependent, frequency-integrated expression for the ring-down signal for a single laser shot is¹²

$$S(t) = \exp\left[-t \frac{c}{\ell}(1-R)\right] \int_{-\infty}^{\infty} d\nu I(\nu - \nu_l) \times \exp\left[-t \frac{c}{\ell} L(\nu - \nu_0)\right]. \quad (1)$$

The exponential outside the integrand simply accounts for the light loss that is due to the less than perfect mirror reflectivities (R) during the tc/ℓ passes through the cavity (t is time, c is the speed of light, and ℓ is the cavity length). Inside the integrand, $I(\nu - \nu_l)$ represents the spectral distribution of the incident-beam intensity centered at frequency ν_l . $L(\nu - \nu_0)$ is the frequency-dependent loss per pass that is due to absorption, which is given by

$$L(\nu - \nu_0) = n\ell S f(\nu - \nu_0), \quad (2)$$

where n is the total number density of the absorber, S is the line strength, and $f(\nu - \nu_0)$ is the integral-normalized absorption line shape centered at frequency ν_0 . The integration in Eq. (1) reflects the fact that each frequency decays with a unique time constant, and the observed signal is a weighted summation of all these decays. Clearly, if $I(\nu - \nu_l)$ is a delta function or $L(\nu - \nu_0)$ changes slowly over the frequency interval encompassed by $I(\nu - \nu_l)$, then a simple exponential decay results. However, if there are significant variations in the spectral content of the incident laser over the absorption feature, then the measured ring-down signal will be a more complicated function of time.

As CRDS has been commonly implemented, the difficulties associated with finite laser bandwidth have largely been avoided. Typically, a ring-down curve is measured by the digitizing of $S(t)$, and the

total losses are inferred by the fitting of the data to a single exponential.^{1-3,13,14} Absorptionlike spectra are measured by the determination of total losses as a function of laser frequency; the absorptive losses and hence number density are then determined by the subtraction of the mirror losses. Figure 1 displays several ring-down spectra of the O_2 $R(9)$ line taken in this manner (at fixed pressure) using the dye laser. For the three different traces, the losses were inferred by the fitting of $S(t)$ with a single exponential and a simple change of the time window over which the data were fit. As the time window was decreased, the apparent absorptive losses increased by nearly 50% for the windows shown here. This anomaly results because the 1.5-GHz nominal HWHM of the dye laser is much broader than the ~ 450 -MHz HWHM of the absorption feature. The total loss at laser frequencies near the absorption line center are dominated by absorption losses, whereas at laser frequencies far away from the absorption line center the total losses are primarily due to mirror losses. Because the ring-down time associated with absorption is much less than the ring-down associated with mirror losses, significant deviation from simple exponential decay occurs. As the fitting time window is narrowed and placed near $t = 0$ (the beginning of the ring-down curve), a single exponential fit of $S(t)$ is weighted more a favor

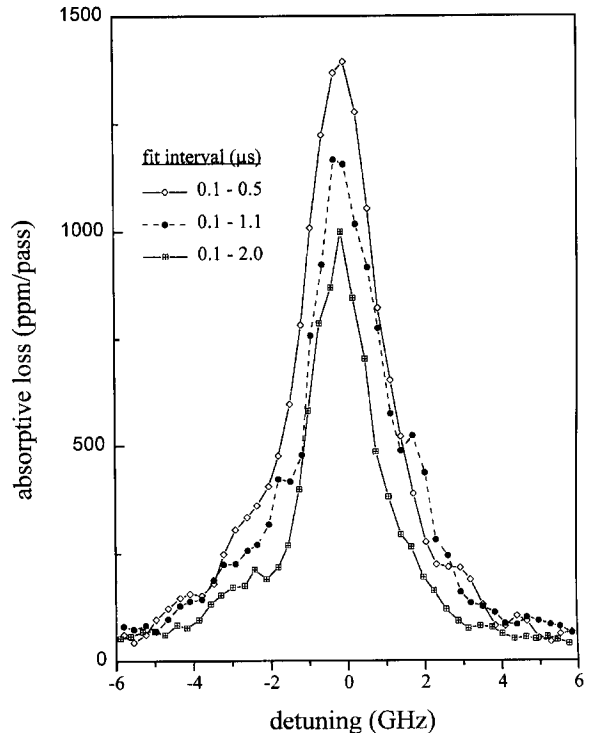


Fig. 1. Ring-down spectrum of the O_2 $R(9)$ line measured with the dye laser. The three traces correspond to three different time windows over which the a single exponential was fit to the measured ring-down signal. Note that as the time window was decreased and placed near $t = 0$, the apparent absorptive losses increased. Expected peak losses for cell condition (1294 Pa, 296.6 K) are 8980 ppm per pass.

of on-resonance light, resulting in increased apparent absorptive losses. In principle, the true losses can be determined by the placement of an infinitely narrow window beginning at $t = 0$. However, in practice, as the window becomes a small fraction of the total decay time, large fluctuations in the inferred losses arise because of scattered light and finite digitization rates.

An obvious way to minimize this difficulty is to use a narrower linewidth laser. Figure 2 shows a ring-down spectrum of the O_2 $\nu R(9)$ transition recorded with a single-mode $Ti:Al_2O_3$ laser (same temperature and pressure as in Fig. 1). With this laser, the apparent absorptive losses determined by a single exponential fit are approximately a factor of 5 to 8 larger than those measured with the dye laser. Furthermore, unlike the dye laser data, changing the fit window does not appreciably change the apparent absorptive losses. But even when this laser is used, the inferred peak absorptive losses (~ 7800 ppm per pass) are well below the expected value of 8980 ppm per pass.⁹

To explore further the origin of these observations, Figs. 3 and 4 show a sum of pulse-energy normalized ring-down signals measured with the dye and the $Ti:Al_2O_3$ lasers at the maximum of the absorption for the $\nu R(9)$ transition for similar conditions as before. The logarithm of the ring-down signal from the dye laser (Fig. 3) is clearly nonlinear with time. This

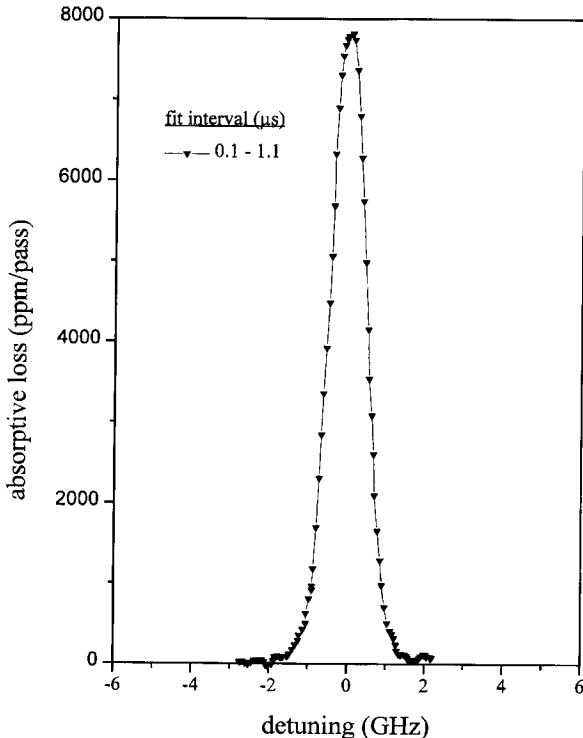


Fig. 2. Ring-down spectrum of the O_2 $\nu R(9)$ line recorded with the $Ti:Al_2O_3$ laser. The losses were determined by a single exponential fit to the ring-down signal over the window shown. Note that the apparent absorptive losses are five to eight times larger than those in Fig. 1. The cell conditions were essentially the same as in Fig. 1.

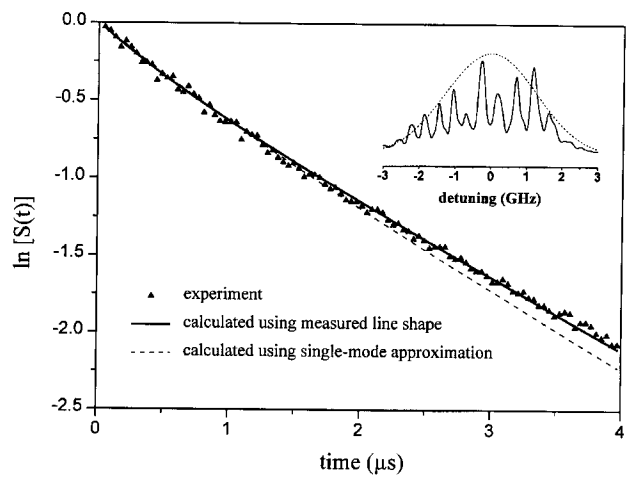


Fig. 3. Ring-down signal as a function of time measured with the dye laser at the peak of the O_2 $\nu R(9)$ transition (\blacktriangle). The measured dye laser spectrum is shown in the inset (solid curve). Also shown in the inset is a single Gaussian (1.5-GHz HWHM) approximation to the laser spectrum (dashed curve). Superimposed on the measured ring-down signal are the calculated ring-down signals with the measured (solid curve) and single-mode Gaussian approximation (dashed curve).

nonlinearity arises, as noted above, because the dye laser spectrum is wide relative to the absorption linewidth. As a result, $S(t)$ comprises a number of different frequency components ringing down with different time constants. The laser's spectrum, summed over 25 laser pulses, is shown in the inset. This highly structured spectrum reflects the longitudinal mode structure of the laser. The relative amplitudes of the modes were observed to vary on a shot-to-shot basis, and corresponding variations in single shot ring-down curves were observed.

Superimposed on the measured ring-down curve in Fig. 3 is a calculated ring-down curve. This curve was calculated with Eqs. (1) and (2), the re-

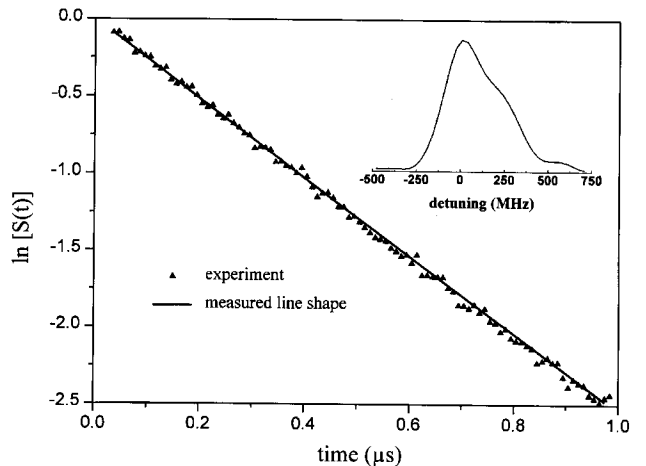


Fig. 4. Ring-down signal as a function of time measured with the $Ti:Al_2O_3$ laser at the peak of the O_2 $\nu R(9)$ transition (\blacktriangle). The measured laser spectrum is shown in the inset. Superimposed on the measured ring-down signal is the ring-down signal calculated with the measured laser spectrum.

ported absorption line-shape parameters and line strength,⁹ the measured temperature and pressure, and the measured laser spectrum shown in the inset. This calculated curve is in good agreement with the measured ring-down signal. Thus one could, in principle, determine the true absorptive losses from a ring-down trace recorded with this instrumentation. However, it must be emphasized that the spectrum shown in the inset does not uniquely determine the ring-down curve; other mode structure and line-strength combinations give equally good fits. Furthermore, large imprecisions in the best-fit absorptive losses arise because the ring-down curve is dominated by the decay of off-resonant light.

Absent a spectrum analyzer with sufficient resolution to measure the detailed mode structure of a dye laser, one might be tempted to approximate the laser line shape by a simple functional form.^{5,13,14} In the spirit of this approach, a ring-down curve, calculated assuming a single 1.5-GHz HWHM Gaussian laser spectral profile, is also shown Fig. 3 (dashed curve). Clearly, this approach yields an unacceptable approximation to the true ring-down curve. The fit can be improved if the absorptive loss per pass is varied by an unrealistically large increase of $\sim 30\%$. The fit can also be improved by a $\sim 15\%$ increase in laser linewidth. However, this effective laser linewidth does not yield a good representation of $S(t)$ for different absorptive losses, and thus absorptivities measured with an effective linewidth will not be linear in number density. Therefore it is concluded that when multimode lasers are used for CRDS, quantitative information can be extracted only when the laser's actual mode structure is taken into account.

In contrast to the signals recorded when the dye laser is used, the natural logarithm of the ring-down signals recorded with the single-mode Ti:Al₂O₃ laser are linear to within signal-to-noise limitations (Fig. 4). The peak absorptive losses inferred from a linear regression to the data in Fig. 4 are 8038 ppm per pass, which is still below the expected value of 9251 ppm per pass. Superimposed on the measured ring-down curve in Fig. 4 is the ring-down curve based on the measured laser line profile (shown in Fig. 4 inset). This calculated curve is in good agreement with the data. By the adjustment of the absorptive losses, a best-fit value of 9110 ppm per pass was obtained. This value is only 1.5% lower than the expected value and well within the estimated experimental uncertainty of $\sim 3\%$. The imprecision in the best-fit absorptive losses is much smaller than the imprecision in the absorptive losses when the dye laser is used. This is because the shape of the ring-down signal recorded with the Ti:Al₂O₃ laser is almost entirely a result of light absorption.

To demonstrate the feasibility of quantitative trace-gas measurements by CRDS, the absorption losses at line center for the ${}^{\circ}R(J)$ ($J = 1, 3, 5, 7, 9, 11, 13, 15, 17, 21, 23$) transitions were determined from

measured ring-down signals obtained with the Ti:Al₂O₃ laser. The absorption losses were determined by the fitting of Eq. (1) to the measured ring-down signals. From the losses, the absolute number densities per rotational quantum state, n_J , were then extracted by the use of the rotational line intensities and the band strength reported in the literature.⁹ The results are presented in Fig. 5 in the form of Boltzmann plot, in which the measured number density per rotational quantum state divided by the state degeneracy $[n_J/(2J+1)]$ is plotted as a function of the state energy.^{7,8} Also shown in this figure (solid line) is the calculated $n_J/(2J+1)$, based on the measured pressure and temperature of the sample cell. The experimental and the calculated values are in excellent agreement. Specifically, when laser linewidth effects are properly accounted for, the best-fit values for $n_J/(2J+1)$ are all within $\sim 5\%$ of the expected value and have an average deviation from the expected values of $\sim 1\%$. The magnitude of the correction was $\sim 12\%$ for the strongest transitions and $\sim 10\%$ for the weaker transitions, and thus the correction is not negligible for the weakest transitions measured here. Furthermore, the sample temperature determined by a linear regression of $n_J/(2J+1)$ versus state energy is 296.2 K, only 0.4 K below the measured sample temperature of 296.6 K. In comparison, the values of $n_J/(2J+1)$ determined from a simple exponential fit to $S(t)$ are, on average, $\sim 10\%$ lower than expected and yield a sample temperature of 298.4 K, some 1.8 K too high. Thus neglecting finite bandwidth effects leads to errors not only in the absolute magnitude of the absorptive losses, but also to nonlinearities with changing number density as well. It should be also noted that for smaller absorption losses the total uncertainties increase, because the fraction of light

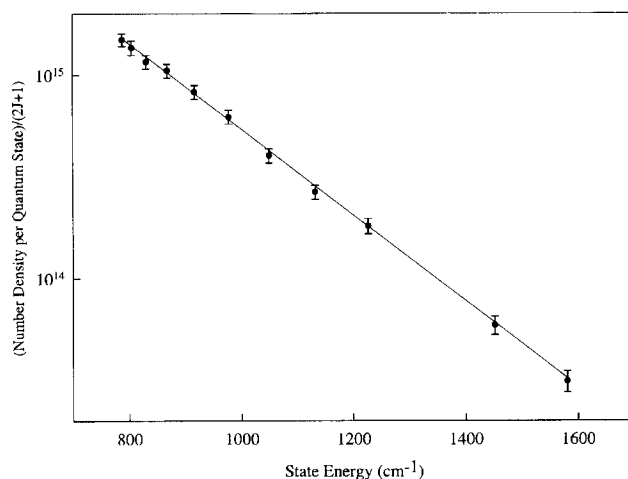


Fig. 5. Number density per rotational quantum state divided by the state degeneracy as a function of state energy, as inferred from the measured ring-down signals and corrected for finite laser bandwidth (\bullet). Also shown (solid line) is the calculated number density per state for the sample cell conditions (1331 Pa, 296.6 K). A linear regression to the data yields a temperature of 296.2 K.

lost through absorption becomes small and the ring-down time on and off resonance approaches the same value. In other words, at low absorption the total uncertainties are dominated by the uncertainty in the determination in the background or mirror losses.

In conclusion, CRDS can indeed be a quantitative spectroscopy when all experimental factors are correctly included in the data analysis. Failure to account for the laser profile leads to systematic errors, and smooth profiles approximating the laser line shape prove to be inadequate. Even if the laser profile is properly taken into account, when the laser's linewidth is comparable with the width of the absorption feature of interest, the accuracy and the sensitivity of the measurement are compromised. We therefore conclude that quantitative CRDS is best achieved by using single-mode, narrow linewidth lasers and by fitting the measured signals to the full time-dependent, frequency-integrated expression for the ring-down signal.

We thank G. T. Fraser for lending us the $\text{Ti:Al}_2\text{O}_3$ laser and G. J. Rosasco for helpful conversations.

References and Notes

1. A. O'Keefe and D. A. G. Deacon, "Cavity ring-down optical spectrometer for absorption measurements using pulsed laser sources," *Rev. Sci. Instrum.* **59**, 2544–2551 (1988).
2. A. O'Keefe, J. J. Scherer, A. L. Cooksy, R. Sheeks, J. Heath, and R. J. Saykally, "Cavity ring-down dye laser spectroscopy of jet-cooled metal clusters: Cu_2 and Cu_3 ," *Chem. Phys. Lett.* **172**, 214–218 (1990).
3. D. Romanini and K. K. Lehmann, "Ring-down cavity absorption spectroscopy of the very weak HCN overtone bands with six, seven, and eight stretching quanta," *J. Chem. Phys.* **99**, 6287–6301 (1993).
4. P. Zalicki and R. N. Zare, "Cavity ring-down spectroscopy for quantitative absorption measurements," *J. Chem. Phys.* **102**, 2708–2717 (1995).
5. R. T. Jongma, M. G. H. Boogaarts, I. Holleman, and G. Meijer, "Trace gas detection with cavity ring-down spectroscopy," *Rev. Sci. Instrum.* **66**, 2821–2828 (1995).
6. This number assumes a 1-m-long cavity, total mirror losses of 1 ppm, a monochromatic laser, and the ability to measure a 1% change in ring-down time. See also G. Rempe, R. J. Thompson, H. J. Kimble, and R. Lalezari, "Measurement of ultralow losses in an optical interferometer," *Opt. Lett.* **17**, 363–365 (1992).
7. H. D. Babcock and L. Herzberg, "Fine structure of the red system of atmospheric oxygen bands," *Astrophys. J.* **108**, 167–190 (1929).
8. K. P. Huber and G. Herzberg, *Molecular Spectra and Molecular Structure* (Van Nostrand, New York, 1979), p. 498.
9. K. J. Ritter and T. D. Wilkerson, "High-resolution spectroscopy of the oxygen A band," *J. Mol. Spectrosc.* **121**, 1–19 (1987).
10. Manufacturers and product names are listed solely for completeness. These specific citations neither constitute an endorsement of the products nor imply that similar products from other companies would be less suitable.
11. For the cavity length (118 cm) and mirror radius of curvature (100 cm) used, light injected into the cavity is not reentrant as the cavity is nonconfocal. However, the observed two-spot pattern can be understood in the context of transverse mode locking; see the discussion of off-axis beam propagation in P. W. Smith, "Mode-locking of lasers," *Proc. IEEE* **58**, 1342–1357 (1970).
12. This formula is Eq. 10 of Zalicki and Zare (Ref. 4), where the summation over cavity modes has been replaced by the corresponding integration. Because the data presented here are time averaged and neither the lasers nor the cavity were stabilized, the use of an integration is believed to be operationally correct.
13. D. L. Huestis, R. A. Copeland, K. Knutsen, T. G. Slinger, R. T. Jongma, M. G. H. Boogaarts, and G. Meijer, "Branch intensities and oscillator strengths for the Herzberg absorption systems in oxygen," *Can. J. Phys.* **72**, 1109 (1994).
14. R. T. Jongma, M. G. H. Boogaarts, and G. Meijer, "Double-resonance spectroscopy on triple states of CO," *J. Mol. Spectrosc.* **165**, 303–314 (1994).